



Dry deposition and desorption of toxic gases to and from snow surfaces

Edvard Karlsson^{*}, Susanne Nyholm

National Defence Research Establishment, NBC Department, S-901 82 Umeå, Sweden

Received 28 October 1997; revised 10 February 1998; accepted 13 February 1998

Abstract

A model describing toxic gas deposition to and desorption from a snow surface is presented. The model is based on the assumption that the deposition is caused by an adsorption of the toxic gas to small amounts of liquid water, which exist in the snow at temperatures equal to or below

Abbreviations: A_c , area of the walls of the test chamber, m^2 ; A_s , area of the snow cover in the test chamber, m^2 ; a , constant in Eq. (18) for r_m ; c_g , gas concentration, $kg\ m^{-3}$; c_{gs} , saturated gas concentration, $kg\ m^{-3}$; c_l , solution concentration, $kg\ m^{-3}$; c_t , total concentration $kg\ m^{-3}$; E , turbulent kinetic energy of the air in the test chamber, $m^2\ s^{-2}$; F , flux of agent (vertical), $kg\ m^{-2}\ s^{-1}$; $H = c_{gs}/S$, Henry's law constant in non-dimensional form; k , von Karmans constant; k_a , air exchange in test chamber caused by the AP2C, s^{-1} ; K_g , molecular vapour diffusion coefficient, $m^2\ s^{-1}$; K_l , molecular liquid diffusion coefficient, $m^2\ s^{-1}$; K_g^s , molecular vapour diffusion coefficient in the pores of the snow, $m^2\ s^{-1}$; K_l^s , molecular liquid diffusion coefficient in the pores of the snow, $m^2\ s^{-1}$; K_e^s , effective diffusion coefficient in the pores of the snow, $m^2\ s^{-1}$; l , distance between transmitters and receivers in ultrasonic turbulence instrument, m; L , Obukov's length, m; q , typical turbulent velocity in the test chamber, $m\ s^{-1}$; R_g , partition coefficient relating total concentration to gas phase concentration; R_l , partition coefficient relating total concentration to solution concentration; r_a , aerodynamic resistance depending on the atmospheric turbulent transfer, $s\ m^{-1}$; r_m , molecular resistance in the atmospheric viscous sub-layer, $s\ m^{-1}$; r_s , surface resistance of the snow depending on the flux into the snow layer, $s\ m^{-1}$; r_s^m , model calculated surface resistance, $s\ m^{-1}$; r_s^{exp} , experimentally measured surface resistance, $s\ m^{-1}$; S , agent solubility in water, $kg\ m^{-3}$; t , time, s; u_* , friction velocity, $m\ s^{-1}$; v_d , dry deposition velocity, $m\ s^{-1}$; $v_{d,c}$, dry deposition velocity onto the walls of the test chamber, $m\ s^{-1}$; $v_{d,c}^{exp}$, measured dry deposition velocity onto snow, $m\ s^{-1}$; Vol, volume of test chamber, m^3 ; V_w , convective velocity (vertical) of the liquid water, $m\ s^{-1}$; V_c , effective convective velocity (vertical) of the liquid water, $m\ s^{-1}$; x , function in expression for Ψ_m ; z , height, m; z_0 , roughness height, m; z_1 , reference height for gas concentration in the atmosphere, m; z_2 , reference height for wind velocity in the atmosphere, m; Δt , time interval when determining $v_{d,c}^{exp}$, s; ϵ , total porosity, $m^3\ m^{-3}$; ϕ , fractional volume of the snow pack that is liquid water, $m^3\ m^{-3}$; μ , first order degradation coefficient, s^{-1} ; θ , fractional volume of the snow pack that is air, $m^3\ m^{-3}$; ν , kinematic viscosity of the air, $m^2\ s^{-1}$; Ψ_c , function in Eq. (17) for r_a ; Ψ_m , function in Eq. (19) for u_*

^{*} Corresponding author. E-mail: karlsson@ume.foa.se

0°C. It includes molecular diffusion in the snow, partition between gas and solution by use of Henry's law, drainage flow in melting snow and decomposition of agent. The interface to the atmosphere is defined by the flux to and from the surface with help of the aerodynamic resistance and the resistance in the viscous sub-layer. Deposition velocities to snow for some air pollutants are reviewed. The model is compared with sarin experiments in a test chamber, which verifies two main features of the model—primarily decreasing deposition with time and decreasing deposition with decreasing temperature. The model shows that the accumulation of sarin in the top layer of snow could be high enough to give lethal or severe injuries to people if the snow was used as drinking water. However, there is a tendency of the model to give too low deposition (too high surface resistance). Possible reasons for this observation are discussed. © 1998 Elsevier Science B.V. All rights reserved.

Keywords: Deposition; Desorption; Snow; Toxic gas; Nerve agent; Sarin

1. Introduction

The removal of gases from the atmosphere by dry deposition to a surface is one of the main processes by which the atmosphere is cleansed of pollutants. Dry deposition of an agent refers to the combined effects of three transfer steps: (1) transfer through the turbulent layer of the atmosphere, (2) molecular transfer through the viscous layer close to the surface, and (3) transfer to the surface as a result of adsorption, dissolution in water or other processes. Most studies have been devoted to measuring and modelling dry deposition of the common air pollutants to vegetation and soil (e.g. Refs. [1–3]), however there is little work devoted to dry deposition to snow. Valdez et al. [4] experimentally studied the deposition of SO₂ and NO₂ onto snow at 20–140 ppb by a chamber method in the laboratory. They found the dry deposition velocity, v_d , to be influenced by liquid water content of the snow pack, snow density, degree of metamorphism, sun light and temperature. The most important single parameter was the liquid water-to-air ratio in the snow. For SO₂, they found a mean deposition velocity of 0.09 cm s⁻¹ for snow at 0°C and 0.04 cm s⁻¹ for snow at temperatures below 0°C. The deposition velocity was lower (0.02 cm⁻¹) for cold dry old metamorphosed snow, compared to newer snow (0.05 cm s⁻¹) at the same temperature. The deposition decreased for longer exposure times and the penetration was 7 cm in cold snow and 4 cm in snow close to 0°C. However, in melting snow with water drainage, there was deeper penetration. Measurements of the deposition velocity for NO₂ gave values 0.005–0.012 cm s⁻¹. Johansson and Granath [5] measured the deposition of gaseous HNO₃ to snow at 6–15 μg m⁻³ in a laboratory chamber and they concluded that the deposition velocities depend on the temperature. They found v_d to be 0.02 cm s⁻¹ at temperatures of -18°C, 0.1 cm s⁻¹ at -3°C, and 0.6 cm s⁻¹ at -2°C. At temperatures of -3°C and lower, the deposition was controlled by the surface resistance; however, at -2°C aerodynamic resistance also contributed significantly to the total resistance. In these experiments the snow layers were only 0.5 cm thick, which is probably not enough to give representative results. Several other investigations [6–11] give similar results, see Table 1.

Table 1
Measured dry deposition velocities on snow

Agent	Concentration in the air	Deposition about 0°C	Velocity cm s ⁻¹ < -2°C	References
SO ₂	20–140 ppb	0.09	0.04	Valdez et al. [4]
	3–7 ppb	> 0.1	0.1	Granath and Johansson [6]
	9–13 ppb	–	0.1	Doveland and Eliassen [7]
	2 ppb	0.15	0.06	Cadle et al. [8]
	Not presented	0–0.15 ^a	0–0.15 ^a	Padro [12]
NO ₂	20–140 ppb	0.01	0.005	Valdez et al. [4]
	6–30 ppb	< 0.03	< 0.03	Granath and Johansson [6]
	Not presented	0.09 ^a	0.09 ^a	Stocker et al. (morning values) [11]
NO	Not presented	0–0.15 ^a	0–0.15 ^a	Padro [10]
	6–30 ppb	< 0.03	< 0.03	Granath and Johansson [6]
HNO ₃	6–15 μg m ⁻³	0.6	0.02–0.1	Johansson and Granath [5]
	0.6 μg m ⁻³	1.4 ^a	1.4 ^a –	Cadle et al. [8]
	Not presented	0.88–3.79	–	Cress et al. [9]
O ₃	40–55 ppb	0.05–0.25	0.02–0.15	Stocker et al. [11]

^aMean value for different temperatures.

To summarise available experimental data, it can be concluded that the dry deposition velocities of SO₂, HNO₃ and NO₂ at temperatures below -2°C seem to be controlled by surface resistance and the deposition velocity will be about 0.1 cm s⁻¹ or less. Near 0°C, the surface resistance decreases and the deposition velocity may increase possibly due to increasing amounts of available liquid water.

Regional scale atmospheric chemistry and pollution models give a crude parameterization of the dry deposition of common air pollutants during winter conditions (e.g. [3,12]). However, Bales et al. [13] presented a more detailed physical–chemical model for SO₂ and calculated surface resistance, r_s , by assuming the existence of a bulk liquid water layer on the snow grains at temperatures $\leq 0^\circ\text{C}$. The model incorporates gaseous molecular diffusion downward into the snow pack, air–water partition through Henry's law constant and aqueous-phase chemical conversion of S(IV) to S(VI). A constant gaseous concentration of SO₂ at the surface is assumed. The model gives increased deposition velocities, v_d , for increased values of water content, decreased values of Henry's law constant and an increased diffusion coefficient. The model gives decreased v_d with decreased temperature and increased time. The amount of liquid water in the snow depends on the temperature and snow density, however, the method to determine these amounts is not described in the paper. The model is said to be consistent with experimental measurements (Valdez et al. [4]). The decrease of v_d with time may indicate the movement towards an equilibrium between the concentration in the air and the concentration above the water solution in the snow. Such a balance can especially be expected for agents with no or little decomposition. If the concentration in the air should decrease below the equilibrium concentration, the deposition would be exchanged by a release of agent (desorption) to the atmosphere. These situations could occur for instantaneous puff or short time release of agent. The purpose of this paper is to extend the Bales et al. [13] model for deposition by improving the description of the atmo-

spheric processes in order to allow for a varying gas concentration in the air and desorption from the snow surface. This will make the model more suitable for instantaneous puffs and short time release of toxic gases. The purpose is also to study the influence of drainage water flow in melting snow and to compare r_s from the model with r_s from nerve agent experiments in a test chamber.

2. Model equations

2.1. Transfer to the snow

There are four possibilities for gas phase adsorption to snow: (1) Gas is solved into pure ice, (2) gas and ice form a liquid solution at the interface, (3) gas is adsorbed to the surface of the ice by physical adsorption and (4) gas is dissolved into liquid water, which exists in snow even at temperatures below 0°C. Concerning the first case, it is known that some gases in very special situations can be trapped into ice by forming clathrate hydrates [14]. In the second case, the solution concentration, c_1 , would be c_g/H , where c_g is gas phase concentration and H is Henry's law constant. Assuming ideal solutions, $H = c_{gs}/S$, where S is solubility and c_{gs} is saturated gas concentration. If this process exists, the freezing point of the solution with the concentration c_g/H must be so low ($\ll 0^\circ\text{C}$) that the liquid solution can exist. This may be observed for highly soluble agents at high gas concentration (c_g), however for many pollutants, H is too high and/or c_g is too low. For example, c_{gs} for the nerve agent sarin at -10°C is $2 \times 10^{-3} \text{ kg m}^{-3}$ and S is 1100 kg m^{-3} (assumed to be the same value as for 0°C). This will give $H = 1.8 \times 10^{-6}$. For a situation with c_g equal to $10 \times 10^{-6} \text{ kg m}^{-3}$, c_1 would then be 5.5 kg m^{-3} , which is a solution of 0.55% per weight sarin. Such a dilute solution is expected to have a freezing point just below 0°C and the solution cannot be formed at -10°C . Thus the second case appears not to be the process for gas phase deposition to snow for many pollutants. Concerning the third case, it is known that gas may adsorb on solid surfaces and there are theories on the process, such as the Langmuir theory [15]. According to the theory, one would expect the deposition to increase with decreasing temperature, but this is contradicted by observations in Table 1. However Conklin et al. [16] found that physical adsorption is dominating at temperatures at and below -30°C , and Sommerfield et al. [17] found physical adsorption dominating below -10°C . Concerning the fourth case, there are many indications [13,18,19] that liquid water exists in snow at temperatures below 0°C . The largest amounts of water exist at 0°C and the amount decreases with decreasing temperatures, which would give decreasing deposition with decreasing temperature. Bales et al. [13] used this principle in a model for SO_2 deposition to snow and they found good correlation with their experimental data. Of the four possibilities, the most probable process appears to be number 4. Therefore, the model of the uptake of agents within the snow pack will be based on the assumption that there exists a bulk liquid water layer on the snow grains even at temperatures below 0°C . The total concentration, c_t , in the snow pack is then formulated as:

$$c_t = \theta c_g + \phi c_1 \quad (1)$$

Table 2

Fractional volumes and water-to-air volume ratio in snow based on Bales et al. [13]

Snow condition	Density, kg m ⁻³	Water content, ϕ	Air content, θ	ϕ/θ
<i>New snow</i>				
Very cold ($\leq -25^\circ\text{C}$)	100	0.00001	0.89	0.000011
Cold (-15°C)	100	0.0001	0.89	0.00011
Warm (-5°C)	100	0.001	0.89	0.001
Melting ^a (0°C)	100	0.01	0.89	0.011
<i>Old snow</i>				
Very cold ($\leq -25^\circ\text{C}$)	400	0.00004	0.57	0.00007
Cold (-15°C)	400	0.0004	0.57	0.0007
Warm (-5°C)	400	0.004	0.57	0.007
Melting ^a (0°C)	400	0.04	0.57	0.07

^aIf there is a drainage flow, ϕ is 2 times the values in the table.

where c_g and c_l are gas and solution concentrations, θ is fractional volume of the snow pack that is air and ϕ is the corresponding volume for liquid water. Assuming equilibrium a relationship between gas and liquid concentrations is given by Henry's law:

$$c_g = Hc_l. \quad (2)$$

The fractional volume of liquid water, ϕ , is assumed to depend on temperature and density and varies over several orders of magnitude. Table 2 gives values of ϕ and θ , and ϕ/θ based on the considerations by Bales et al. [13], who defined the snow conditions in terms of 'very cold', 'cold', 'warm' and 'melting'. We have defined 'very cold' as temperatures $\leq -25^\circ\text{C}$, 'cold' as temperature equal to -15°C , 'warm' as temperature equal to -5°C and 'melting' as temperature equal to 0°C . For values in-between those given in Table 2, a linear interpolation was made. There are probably some uncertainties in the values of ϕ . Since ϕ decreases with decreasing temperature, the deposition will also decrease (the resistance will increase) with decreasing temperature.

2.2. Surface resistance, r_s and fluxes to and in the snow

Since r_s largely depends on the snow conditions, r_s is used when comparing the model results with experiments. The model calculated surface resistance r_s^m is achieved from the definition of dry deposition velocity, v_d [20]:

$$v_d = \frac{1}{r_a + r_m + r_s}. \quad (3)$$

where r_a is the aerodynamic resistance depending on the atmospheric turbulent transfer, r_m is the molecular resistance in the atmospheric viscous sub-layer and r_s is the surface resistance of the snow, which depends on the flux into the snow layer. The dry

deposition flux, $F(z = 0, t)$, to the surface is needed in order to calculate r_s^m . According to Zannetti [20]:

$$|F(z = 0, t)| = v_d(z_1) c_g(z_1, t) \tag{4}$$

where $c_g(z_1)$ is gas concentration at some reference height, z_1 , in the atmosphere. Notice that the dry deposition flux is defined to be ≥ 0 in Eq. (4). If $c_g(z_1)$ is known and $F(z = 0, t)$, r_a and r_m are calculated by the model, r_s^m can be solved for the case of deposition from Eqs. (3) and (4):

$$r_s^m = \frac{c_g(z_1, t)}{|F(z = 0, t)|} - r_a - r_m. \tag{5}$$

However, in our model we also take into account possible desorption from snow to the atmosphere. Thus, the flux formulation must be general, allowing transfer both upwards and downwards. Similar to a model by Jury et al. [21] for evaporation of chemicals in the soil, the flux of agent in the snow pack is assumed to be one-dimensional and occur through gaseous molecular diffusion, liquid molecular diffusion and convection of solution. Therefore, other possible transfer processes such as transfer caused by pressure variations, are excluded. The flux equation can then be written:

$$F = -K_g^s \frac{\partial c_g}{\partial z} - K_l^s \frac{\partial c_l}{\partial z} + V_w c_l \tag{6}$$

where K_g^s and K_l^s are vapour and liquid diffusion coefficients in the pores, modified to take into account the reduced flow area and increased path length of the molecules in the pores of the snow and V_w is the convective velocity of the liquid water, also modified for the reduced flow area. There are several ways of formulating K_g^s and K_l^s . The theory proposed by Millington [22] and used by Jury et al. [21] is adopted here. According to this theory, the area of pore space exposed in a cut surface is equal to $\varepsilon m^2 m^{-2}$ if $\varepsilon m^3 m^{-3}$ is the total porosity. However, the effective area for transfer depends on the interaction of pores at two different planes, resulting in an effective area which is less than ε . Assuming an isotropic porous medium with spherical pores, it can be shown that the effective area is $\varepsilon^{4/3}$. Thus, if only gas or liquid occupies the pores $(K_g^s)/(K_g) = \varepsilon^{4/3}$ or $(K_l^s)/(K_l) = \varepsilon^{4/3}$. In a similar way, the effect of both gas and liquid can be derived giving:

$$K_g^s = \frac{\theta^{10/3}}{(\theta + \phi)^2} K_g \text{ and } K_l^s = \frac{\phi^{10/3}}{(\theta + \phi)^2} K_l \tag{7}$$

where $\theta + \phi = \varepsilon$, K_g are K_l are the normal molecular diffusion coefficients. By using Eqs. (1) and (2), the total concentration, c_t , can be expressed as:

$$c_t = R_1 c_1 = R_g c_g, \tag{8}$$

where

$$R_1 = \theta H + \phi, \tag{9}$$

$$R_g = \theta + \frac{\phi}{H}. \tag{10}$$

The flux Eq. (6) can then be formulated as:

$$F = -K_e^s \frac{\partial c_t}{\partial z} + V_e c_t \quad (11)$$

where K_e^s is an effective diffusion coefficient and V_e is an effective convection velocity:

$$K_e^s = \frac{K_g^s}{R_g} + \frac{K_l^s}{R_l}, \quad (12)$$

$$V_e = \frac{V_w}{R_l}. \quad (13)$$

2.3. Mass balance equation

In a one-dimensional homogeneous porous medium, the change of total concentration, c_t , for a single agent undergoing first-order decay is:

$$\frac{\partial c_t}{\partial t} = -\frac{\partial F}{\partial z} - \mu c_t, \quad (14)$$

$$\frac{\partial c_t}{\partial t} = K_e^s \frac{\partial^2 c_t}{\partial z^2} - V_e \frac{\partial c_t}{\partial z} - \mu c_t, \quad (15)$$

where t is the time variable, z is the depth variable and μ is a degradation coefficient (s^{-1}).

2.4. Upper boundary condition and calculation of r_a and r_m

The flux to and from the surface is formulated to allow both deposition and desorption and is determined by the molecular and the turbulent transfer according to Zannetti [20]:

$$F(z=0,t) = -\frac{c_g(z_1,t) - c_g(z=0,t)}{r_a + r_m} \quad (16)$$

where,

$$r_a = \frac{l}{ku_*} \left(\ln \frac{z_1}{z_0} - \Psi_c \left(\frac{z_1}{L} \right) \right), \quad (17)$$

u_* is friction velocity, $\Psi_c = 0$ for neutral stratification, $\Psi_c = 2 \ln \left(0.5 \left(1 + \sqrt{1 - \frac{16z_1}{L}} \right) \right)$ for unstable stratification, $\Psi_c = -5z_1/L$ for stable stratification; L is Obukov's length, z_1 is reference height for gas concentration in the atmosphere.

$$r_m = a \frac{\left(\frac{\nu}{K_g} \right)^{2/3}}{ku_*}, \quad (18)$$

where a is a constant, which is assumed to be 2.0, ν is the kinematic viscosity of the air and $k = 0.4$ is von Karman's constant. The friction velocity depends on wind velocity and atmospheric stability according to:

$$u_* = \frac{ku(z_2)}{\ln \frac{z_2}{z_0} \Psi_m(z_2/L)} \quad (19)$$

where $\Psi_m = 0$ for neutral stratification, $\Psi_m = \ln\left[\frac{(1+x^2)/(2)}{(1+x)/(2)}\right]^2 - \arctan x + \pi/2$ with $x = (1-16z_2/L)^{1/4}$ for unstable stratification, $\Psi_m = -5z_2/L$ for stable stratification; z_0 is the roughness height and z_2 is the reference height for wind velocity.

2.5. Lower boundary

$$c_g(z = -\infty, t) = 0. \quad (20)$$

2.6. Numerical method

The differential Eq. (15) is solved using finite differences with a semi-implicit scheme similar to Crank–Nicolson's method [23]. The time step was 0.3–1.0 s and the grid distance in the snow was 0.1–0.01 cm. To confirm the numerical solution, a comparison was made with an analytical solution for a simple case presented by Karlsson [24].

3. Experiments

The model is compared with nerve agent experiments previously reported by Karlsson et al. [25]. Since r_s largely depends on the snow conditions, the comparison is made for r_s . A sealed glass test chamber ($1.2 \times 1.2 \times 1.2 \text{ m}^3$) coated with silicon to minimize gas deposition was prepared and placed in a cold-storage room. The bottom part of the test chamber could be taken outdoors. Before the experiments started, snow from the upper layer of the natural snow cover was gently transferred to the bottom part with a spade giving a 15 cm thick snow layer. Then, the bottom part was attached to the test chamber and sealed.

Snow density, snow temperature, air temperature, air humidity and concentration of nerve agent sarin were measured. An AP2C instrument [26] supplied by GIAT Industries was used for the sarin measurements. In each trial, approximately 20 mg of sarin was injected through a small opening onto a heated glass encapsulated thermistor at

temperature $\leq 100^\circ\text{C}$. The sarin evaporated in 10–20 s and the expected initial concentration in the air is estimated to be about 13 mg m^{-3} . However, the initial concentration was measured in the range of $5\text{--}10 \text{ mg m}^{-3}$, probably due to degradation during vaporisation. Every second experiment was a control, without snow, to check both the behaviour of the test chamber and to measure the deposition of sarin on the chamber walls.

A 36 W electric fan with a flow area of 0.013 m^2 giving an air stream of maximum velocity of about 10 m s^{-1} generated turbulence, which gave an atmospheric resistance ($r_a + r_m$) similar to values existing outdoor. Different positions of the fan were tested and flow and turbulent kinetic energy, E , were measured at different points with a Solent ultrasonic research turbulence instrument [27] with a sampling frequency of 20 Hz and distance, l , $\approx 0.1 \text{ m}$, between transmitters and receivers. When the fan was started in a new position and stationary condition was achieved, the measurements started with 5 min averaging time. A position in the centre of the box, with the flow going upwards, generated the most homogenous turbulence and the least swirling motion in the lower part of the test chamber. The missing turbulent energy caused by cutting off wave numbers larger than $1/l \approx 10 \text{ m}^{-1}$ was about 20%. This estimate was made by integrating the energy spectrum which was assumed to be proportional to wave number raised to $-5/3$ according to the theory of Kolmogoroff for inertial subrange. The swirling flow was about 0.3 m s^{-1} . The atmospheric resistance ($r_a + r_m$) was determined by measuring the evaporation rate (F) of water in a petri dish at room temperature and applying Eq. (16), with $c_g(z=0,t)$ equal to the saturation concentration, c_{gs} . The sum of the resistances ($r_a + r_m$) for water was 150 s m^{-1} . Eq. (18) was used to estimate r_m . Since u_* could not be measured, it was replaced by a typical turbulent velocity, q , which was determined by using the measured turbulent kinetic energy, E . Subsequently, q was calculated according to $q = \sqrt{2E}$ and varied between 0.32 and 0.45 m s^{-1} in the lower part of the test chamber with mean value 0.39 m s^{-1} . Eq. (18) gave r_m equal to 10 s m^{-1} and 25 s m^{-1} for water and sarin (at 0°C), respectively. Thus, r_a was 140 s m^{-1} . Molecular diffusion coefficients decrease with decreasing temperature [28]; therefore, r_m for sarin will be 10% larger at -15°C than at 0°C . There is some influence on r_m from the swirling velocity and the missing turbulent energy. However, r_a is the transport limited atmospheric parameter since $r_a > r_m$ and therefore some inaccuracy in the determination of r_m will only give minor influence on the transfer of vapour and the determination of r_s .

Four experiments were performed with melting snow and the test chamber temperature of approximately $+1^\circ\text{C}$. Three experiments were performed at test chamber temperature of about $+1^\circ\text{C}$, however, the snow temperature was $\leq 0^\circ\text{C}$. Four experiments were performed with test chamber temperature equal to -15°C and with snow temperature in the range of $-10\text{--}-15^\circ\text{C}$. A typical example of the measured phosphorus concentration is illustrated in Fig. 1. In the experiments with temperatures at $-10\text{--}-15^\circ\text{C}$, the deposition caused the sarin concentration to decrease to 10% of the initial value within 2 h. At 0°C , the same decrease in concentration occurred within approximately 15–30 min. Thus, a decrease of deposition velocity (increase of resistance) with decreasing temperature was observed, and this verifies one main feature of the model (see Section 2.1).

Temperature -15 C.

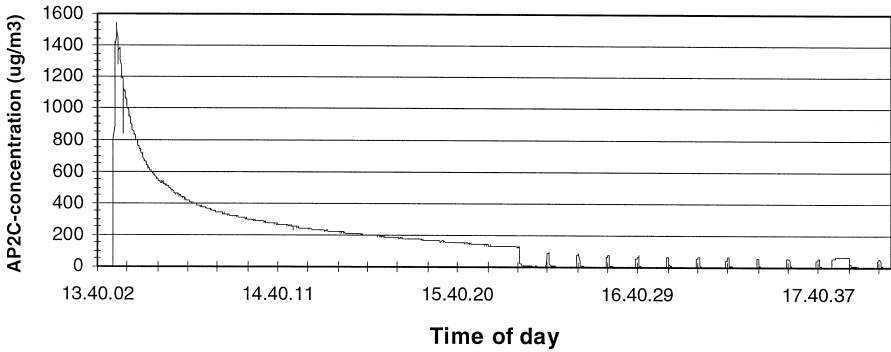


Fig. 1. Example of phosphorus concentrations measured by the AP2C instrument at a temperature of -15°C . The concentration of sarin is obtained by multiplying with 4.52. After 16 h, the samples were taken over 1 min every 10 min.

The deposition velocity was calculated with the assumption that the air was well mixed in the test chamber giving:

$$v_d^{\text{exp}} = \frac{\text{Vol}}{A_s} \left(-\frac{\ln \frac{c_g(t)}{c_g(t-\Delta t)}}{\Delta t} - k_a - \frac{v_{d_c} A_c}{\text{Vol}} \right) \quad (21)$$

where, v_d^{exp} is measured deposition velocity onto snow, A_s is area of the snow cover, Vol is volume of test chamber, t is time from release, c_g is concentration at time t , k_a is air exchange caused by the AP2C, v_{d_c} is deposition velocity onto the walls of the test chamber and A_c is area of the walls and ceiling of the test chamber. Δt was between 1.5 and 10 min, depending on the rate that the sarin concentration decreased in the test chamber. v_{d_c} , which was determined in the control experiments without snow, was very low (mean value about $3 \times 10^{-6} \text{ m s}^{-1}$) when compared to the observed deposition velocity to the snow (10^{-2} – 10^{-4} m s^{-1}). The surface resistance of the snow, r_s^{exp} , was calculated from Eq. (3) according:

$$r_s^{\text{exp}} = \frac{1}{v_d^{\text{exp}}} - r_a - r_m. \quad (22)$$

4. Comparison between surface resistances, r_s , from the model and the experiments

In Fig. 2, the observed surface resistance, r_s^{exp} , of nerve agent sarin (Eq. (22)) is compared with model calculated surface resistance, r_s^{m} (Eq. (5)), after solving the model Eqs. (15), (16) and (20) for the conditions in the test chamber. The concentration of sarin in the air, $c_g(z_1, t)$, required for the upper boundary Eq. (16), was taken from the

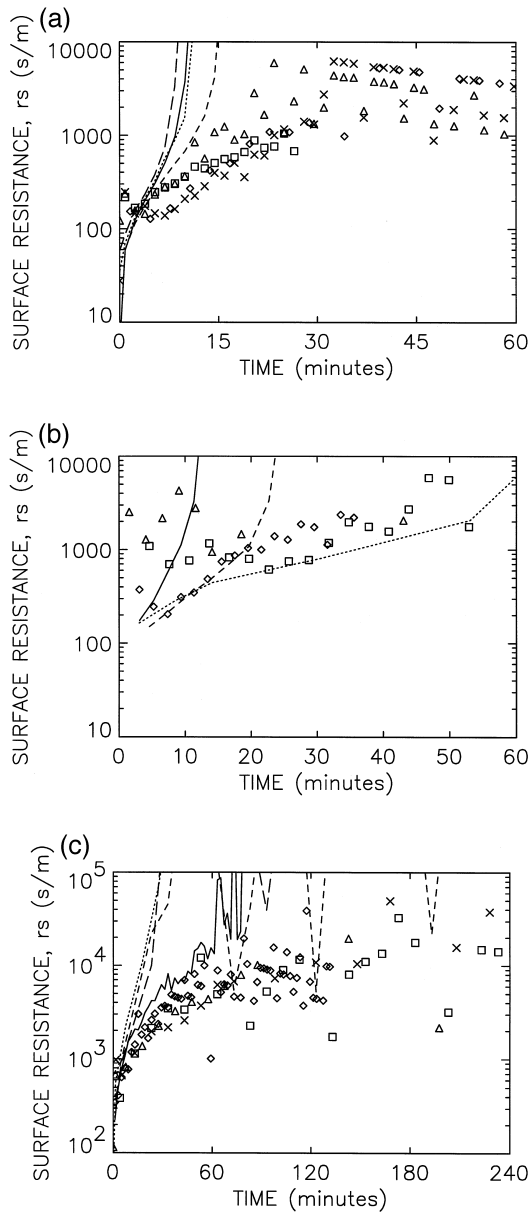


Fig. 2. Model calculated (lines) and measured (symbols) surface resistances, r_s , of sarin in the test chamber at three temperatures. The 3–4 experiments and corresponding model simulations are designed as: \diamond ———, Δ ·····, \square ---, \times —·—·—. (a) Four experiments with melting snow at 0°C with test chamber temperatures +1°C; (b) three experiments with test chamber temperature +1°C and snow at 0 to -2°C; and (c) four experiments with test chamber temperature -15°C and snow in the range of -10 to -15°C. Experimental variables and model parameters in the test chamber are listed in Tables 2 and 3.

Table 3

Experimental variables and model parameters in the test chamber for Fig. 2

Variable	Fig. 2a	Fig. 2b	Fig. 2c
Snow temperature, °C	0, melting	0 to -2	-10 to -15
Test chamber temperature, °C	≈ 1	≈ 1	-15
Snow density, kg m ⁻³	230–360	150–260	130–160
Water solubility ^a , <i>S</i> , kg m ⁻³ , [29]	1100	1100	1100
Saturation concentration, <i>c</i> _{gs} , kg m ⁻³ , [30,31]	4288 × 10 ⁻⁶	4000 × 10 ⁻⁶	1400–2200 × 10 ⁻⁶
Henry's law constant, <i>H</i> = <i>c</i> _{gs} / <i>S</i>	3.9 × 10 ⁻⁶	3.6 × 10 ⁻⁶	1.3–2.0 × 10 ⁻⁶
Diffusion coefficient in air, <i>K</i> _g , m ² s ⁻¹ , [28]	6.2 × 10 ⁻⁶	6.2 × 10 ⁻⁶	5.6 × 10 ⁻⁶
Diffusion coefficient in water, <i>K</i> ₁ , m ² s ⁻¹ , [28]	5.0 × 10 ⁻¹⁰	5.0 × 10 ⁻¹⁰	5.0 × 10 ⁻¹⁰
Degradation coefficient, <i>μ</i> , s ⁻¹ , [32]	2 × 10 ^{-7c}	2 × 10 ^{-7c}	2 × 10 ^{-7c}
Drainage water flow velocity ^b , <i>V</i> _w , m s ⁻¹	0	0	0
Aerodynamic resistance, <i>r</i> _a , s m ⁻¹	140	140	140
Resistance in the viscous sub-layer, <i>r</i> _m , s m ⁻¹	25	25	30
Measured concentration, <i>c</i> _g (<i>z</i> ₁), in test chamber, kg m ⁻³	0 – ≈ 8 × 10 ⁻⁶	0 – ≈ 6 × 10 ⁻⁶	0 – ≈ 7 × 10 ⁻⁶
Number of experiments	4	3	4

^aSarin is infinitely miscible with water, which means that *S* is equal to the liquid density.

^bNo drainage flow was assumed, see text.

^cCorresponding to a buffered solution of pH 4.4, which is the mean pH-value of snow precipitation in Umeå, where the snow samples were taken [33].

measurements. In this way, the effect of deposition/desorption to/from the walls is included in the model calculations. Liquid water content, ϕ , and air content, θ , were taken from Table 2 and other model parameters from Table 3. For snow temperatures < 0°C it was natural to assume the drainage flow V_w to be zero. However, for melting snow there may be a drainage flow with $V_w \neq 0$. In order to test the same formulation as Bales et al. [13], no drainage flow was assumed in Fig. 2, but in Fig. 3 the effect of $V_w \neq 0$ was studied. The input data for the three to four cases in Fig may differ a little concerning snow density, snow temperature and $c_g(z_1, t)$, resulting in some differences between the individual model simulations. In order to reduce the air exchange of the test

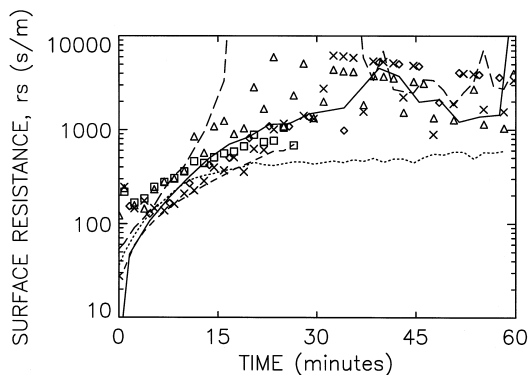


Fig. 3. Same conditions as Fig. 2a, except that the model parameters are modified according to: $\phi = 3$ times the value in Table 2; $V_w = -1.75 \times 10^{-8}$ m s⁻¹ and $\mu = 0.5 \times 10^{-4}$ s⁻¹.

chamber in experiments with low temperature and long duration (Fig. 2c), the concentration, $c_g(z_1, t)$, of the test chamber was measured over 1 min every 10 min except for some period in the beginning. A linear interpolation was used to decide $c_g(z_1, t)$ for intermedium times in the model calculation of r_s . Because of delay in the instrument there was also some reduced accuracy in the measurements. However, there were no numerical problems when solving c_i from Eq. (15), but the intervals in the measurements and the reduced accuracy caused small variations of the flux F at the surface. Since r_s depends on $1/F$ (Eq. (5)) this caused a scatter in the model simulation when F was small (Fig. 2c).

Fig. 2a (melting snow) and c (-15°C) show that both the model and experimental values of the surface resistances, r_s , increase with time, thus verifying one main feature of the model (see also Section 5). The model and experimental values are similar in the beginning; however, the model values increase faster than the observations. The latter also showed a tendency to reach a constant value, $\approx 2000 \text{ s m}^{-1}$ in Fig. 2a and $\approx 10000 \text{ s m}^{-1}$ in Fig. 2c, after a period of time. The surface resistance, r_s^m , of the model often approached infinity when $c_g(z_1, t)$ reached a low value. This was often followed by desorption, but is not shown in Fig. 2, since r_s^m would be negative. In Fig. 2b, the increase in the experimental r_s is not as obvious as in Fig. 2a and c, as the values in one of the three experiments were relatively high from the beginning. It is probable that the experiments in Fig. 2b represent a more heterogeneous group, since cold snow was placed in the test chamber at about $+1^\circ\text{C}$. The time prior to the start of the experiments could vary substantially, resulting in different time periods during which the snow was exposed to 0°C . This could produce different quantities of liquid water (ϕ) in the snow. The experiments also verify the increase of r_s with decreasing temperature, since r_s begins and ends at higher values in Fig. 2c (-15°C) than in Fig. 2a (0°C) (see also Sections 2.1, 3 and 5).

It is relatively easy to adopt model parameters ϕ , V_w and μ to give corresponding values between model and experimental results. For example higher values of ϕ would give a smaller slope in the model, since $(dr_s)/(dt)$ is nearly proportional to $(H)/(\phi)$ [24]. Lower values of the saturation concentration, c_{gs} , would also give a smaller slope, since H would be lower. Drainage flow for melting snow and a higher decomposition rate would account for the tendency of r_s to reach a constant value. Fig. 3 shows an example of the adoption of these model parameters for the case shown in Fig. 2a and the rationale for this is discussed in Section 6. In Fig. 3 the model calculation of r_s is influenced by some scatter, caused by interrupts in the measurements of $c_g(z_1, t)$, when the sarin concentration in the cold storage room was checked.

5. Model results

Figs. 2 and 3 show results from the test chamber when the concentration in the air, $c_g(z_1)$, continually decreases with time. In order to illustrate the behaviour of the model for outdoor conditions, where $c_g(z_1)$ is constant or changed rapidly, calculations are made for the nerve agent sarin. Fig. 4 shows total concentrations in the snow after different exposure times at -5°C . Figs. 5 and 6 show the vapour flux to the snow

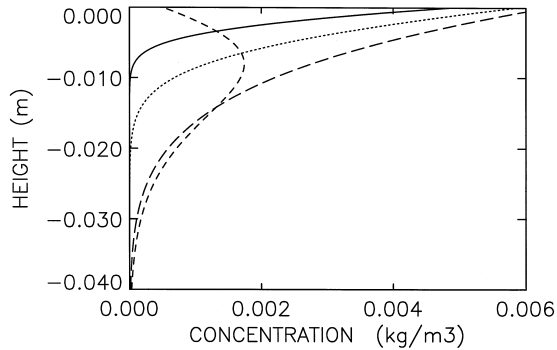


Fig. 4. Calculated total concentrations of nerve agent sarin in snow after 15 min (—), 1 h (···), 4 h (---) and 5 h (-.-). The temperature is -5°C , the snow is newly fallen (density = 100 kg m^{-3}), the wind velocity is 3 m s^{-1} at 10 m and the stratification is stable (Obukov length $L = 40\text{ m}$). The gas concentration, $c_g(z_1)$, in air at 20 m is $10 \times 10^{-6}\text{ kg m}^{-3}$ for 4 h, after which it is reduced to 0 kg m^{-3} . The roughness height is 0.001 m , the degradation coefficient, μ , is $5 \times 10^{-5}\text{ s}^{-1}$ and the draining water flow, V_w , is 0 ms^{-1} . The liquid water content ϕ is two times the value in Table 2.

surface and the surface resistance, r_s , at temperatures 0° , -5° and -15°C . For all figures, the stratification is stable (Obukov length $L = 40\text{ m}$), the wind velocity is 3 m s^{-1} at 10 m and roughness length, z_0 , is 0.001 m . This gave the atmospheric resistance ($r_a + r_m$) equal to $\approx 350\text{ s m}^{-1}$. The concentration, $c_g(z_1)$, in the air at 20 m is $10 \times 10^{-6}\text{ kg m}^{-3}$. Fig. 5 also shows the flux from the snow to the atmosphere as a result of desorption, when the concentration in the air, $c_g(z_1)$, at 20 m is reduced to 0 kg m^{-3} after 4 h.

Fig. 4 shows that a significant amount of sarin is accumulated in the top 1 cm of snow. This amount could give lethal or severe injuries to people [34] if the snow was used as drinking water.

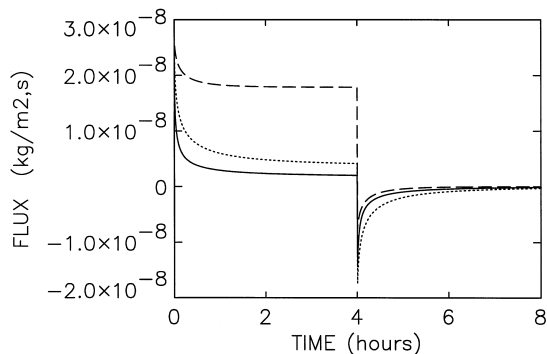


Fig. 5. Model calculated vapour flux of nerve agent sarin to and from (negative flow) the snow surface at temperatures of 0°C (---), -5°C (···) and -15°C (—). The gas concentration, $c_g(z_1)$, in the air at 20 m is $10 \times 10^{-6}\text{ kg m}^{-3}$ for 4 h, after which it is reduced to 0 kg m^{-3} . At 0°C the drainage velocity, V_w , is $-1.75 \times 10^{-8}\text{ m s}^{-1}$ (melting of $\approx 0.25\text{ mm snow h}^{-1}$). Other conditions are the same as in Fig. 4.

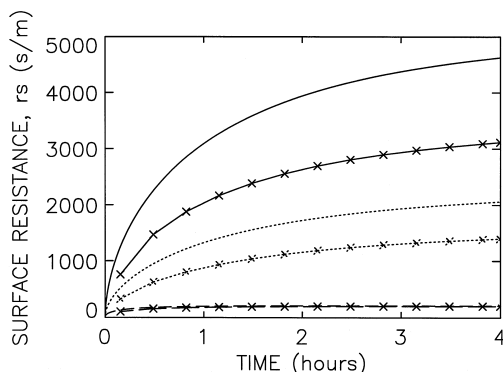


Fig. 6. Calculated surface resistances (r_s) of sarin for new snow and old snow (x) at snow temperatures equal to 0 (---), -5 (···) and -15°C (————). Other conditions are the same as in Figs. 4 and 5.

Fig. 5 shows two main features of the model: (1) the deposition decreases with time, especially in the beginning, and (2) the deposition decreases with decreasing temperature. This also indicates that the surface resistance, r_s , increases with increasing time and decreasing temperature (Fig. 6). The reason for the decrease of flux with time is due to the increase of agent in the snow with time, which will reduce the difference between the gas concentration, $c_g(z_1)$, in the air and the gas concentration, $c_g(z=0)$, at the snow surface (Eq. (16)). The decrease of deposition with decreasing temperature is the result of reduced liquid water (Table 2), which can adsorb the gas while in the air. Figs. 5 and 6 show a large difference between melting snow with large deposition (low r_s) and snow at temperatures below zero with low deposition and a large r_s . For the melting snow r_s is $\leq 173 \text{ s m}^{-1}$ and less than $r_a + r_m$, which is approximately 350 s m^{-1} . Thus, the atmospheric resistance, $r_a + r_m$, is the transport limiting parameter in the chosen weather conditions (compare Eqs. (3) and (4)). For temperatures $< 0^\circ\text{C}$, r_s is larger than $r_a + r_m$ after a relatively short exposure time and r_s will then be the transport limiting parameter. A comparison between Figs. 6 and 3 indicates that a constant concentration ($c_g(z_1)$) in the air gives lower values of r_s than a decreasing $c_g(z_1)$.

The desorption flux is rather similar for all temperatures. It starts with a relatively high value, but decreases with time. Note that r_s has no meaningful definition in the case of desorption, since it is not included in Eq. (16).

6. Discussion and conclusions

The comparison between model and experiments in the test chamber (Fig. 2) shows a tendency of the model to give a higher surface resistance, r_s , (lower deposition) than found in the experiments. However, two–three times higher values of the liquid water content, ϕ , combined with a degradation rate, μ , equal to $5 \times 10^{-5} \text{ s}^{-1}$, and for melting

snow, a drainage flow velocity, V_w , equal to $-1.75 \times 10^{-8} \text{ m s}^{-1}$ gave a better correlation between model and experiment. These values appear reasonable. For example Table 2, based on Bales et al. [13] assumptions, postulates a doubling of ϕ , if there is a drainage flow. The used value of V_w corresponds to melting of about 0.25 mm snow h^{-1} , which seems to be a rather reasonable melting rate. Bales et al. [13] did not specify the method used to determine ϕ and their temperature scale was in terms of drainage, melting, warm, cold and very cold. ϕ probably depends on the amount of pollution and impurities, e.g. sulphur compounds, in the water, which can contribute to a reduced freezing point. These pollutants may have been transferred to the snow by process 2 and 4 discussed in Section 2.1, followed by decomposition, which prevents desorption. It can also be a result of wet deposition during snow fall. Thus, ϕ probably varies substantially depending on the previous history of the snow, and therefore adjustments of the values in Table 2 would be realistic. A reduction of c_{gs} to about 50% of the values used in Table 3, produces the same effect as doubling ϕ . This reduction may be realistic, since reported values of c_{gs} in the literature differ by a factor of 2 [30,35]. A degradation rate, μ , equal to $5 \times 10^{-5} \text{ s}^{-1}$ could exist if the acidifying agents (H_2SO_4 , HNO_3) in the snow are localised to the small amount of liquid water. The pH-value would be lower and the decomposition rate, μ , higher [32]. Hydrolyses products of sarin may also contribute to lowering the pH-value [32]. The results show that drainage flow is an important process influencing deposition and desorption of gases. For SO_2 , methods exist to calculate the degradation (Bales et al. [13]), but in many cases there are uncertainties in how to specify ϕ , V_w and μ . In order to improve the model, a comparison should be performed between the modified model, according to the discussion and independent experiments. In addition, model equations for heat transfer and V_w need to be developed. Improved methods for determining ϕ and μ should include time history of the snow, such as by taking into account impurities and the pH-value of the snow.

Excluded processes may also account for some of the differences between model and experiments. For example physical adsorption (see Section 2.1) may be important at low temperatures [16,17].

The ‘initially missing sarin’, which was assumed to degrade during the release (Section 3), cannot explain the difference between model and experiments in Fig. 2. If the missing agent had instead deposited to the walls of the test chamber in a very fast process, it is probable that the agent had desorbed when the sarin concentration in the test chamber decreased. This would correspond to a higher released amount of sarin and a higher measured deposition (lower resistance), which would give larger difference between model and experiment in Fig. 2. If the ‘initially missing sarin’ had deposited to the snow in a very fast process, there would have been an initial sarin concentration in the snow. If this is introduced in the model, the deposition would be reduced (the resistance would increase) with a larger difference between model and experiments in Fig. 2. Pressure driven transfer, which was excluded in the derivation of the model (Section 2.2), appears to be unable to explain the differences in Fig. 2, since such a process would increase both the deposition and the desorption. The amount of liquid water, ϕ , is small for temperatures below 0°C , resulting in a small value of K_1^s . Because of the small amount of ϕ , K_g^s will approach Millington’s [22] original formulation for

diffusion when the pores contain only gas: $K_g^s = \varepsilon^{4/3}$, which probably means a relatively good accuracy for K_g^s . For situations with higher ϕ , there exists alternative formulations [36] taking into account that mass transfer is possible either by parallel diffusion through pores filled completely with gas or a liquid, or serial diffusion through gas- and liquid-filled regions. Therefore, a comparison between different formulations would be valuable.

The spread of the experimental data points in Figs. 2 and 3 may depend on snow conditions, which are not taken into account, e.g. the diameters of the pores. There is also a tendency for increasing spread with time, probably depending on reduced measuring accuracy at low concentrations in the test chamber (compare Fig. 1).

The main features of the model are: (1) the deposition decreases (r_s increases) with time, (2) the deposition decreases (r_s increases) with decreasing temperature, (3) the deposition increases (r_s decreases) with the age (density) of the snow, (4) deposition is changed to desorption when the gas concentration in the air drops significantly and (5) the desorption decreases with time. The decrease of the deposition (increase of r_s) with time is very significant initially, implying a large difference in deposition velocity between an instantaneous puff giving a short exposure time and a continuous plume giving a long exposure time. The model shows that the accumulation of sarin in the top layer of snow is so high, that it can cause lethal or severe injuries to people if the snow was used to drinking water. Test chamber experiments verify the increase of r_s with increasing time and decreasing temperature.

Acknowledgements

We are grateful to Dr. Jakob Noreland, Prof. Dr. Sergej Zilitinkevich and Mr. Otto Grafner for critical review of the manuscript, to Dr. Bo Koch and Dr. Åsa Edvinsson for discussions on toxicological effects of sarin and to Mr. Tage Berglund and Mr. Melker Nordstrand for supplying experimental data.

References

- [1] A.C. Chamberlin, Aspects of the deposition of radioactive and other gases and particles, *Int. J. Air Pollut.* 3 (1969) 63–88.
- [2] W.G. Slinn, L. Hasse, B.B. Hicks, A.W. Hogan, D. Lal, P.S. Liss, K.O. Munnich, G.A. Sehmel, O. Vittori, Some aspects of the transfer of atmospheric trace constituents past the air–sea interface, *Atmos. Environ.* 15 (1978) 863.
- [3] M.L. Weasley, Parameterization of surface resistances to gaseous dry deposition in regional-scale numerical models, *Atmos. Environ.* 6 (1989) 1293.
- [4] M.P. Valdez, R.C. Bales, D.A. Stanley, G.A. Dawson, Gaseous deposition to snow: 1. Experimental study of SO₂ and NO₂ deposition, *J. Geophys. Res.* 92 (1987) 9779.
- [5] C. Johansson, L. Granath, An experimental study of the dry deposition of gaseous nitric acid to snow, *Atmos. Environ.* 20 (1986) 1165.
- [6] L. Granath, C. Johansson, Dry deposition of SO₂ and NO_x in winter, *Atmos. Environ.* 17 (1983) 191.

- [7] H. Doveland, A. Eliassen, Dry deposition on a snow surface, *Atmos. Environ.* 10 (1976) 783.
- [8] S.H. Cadle, J.M. Dasch, P.A. Mulawa, Atmospheric concentrations and the deposition velocity to snow of nitric acid, sulfur dioxide and various particulate species, *Atmos. Environ.* 19 (1985) 1819.
- [9] R.G. Cress, M.W. Williams, H. Sievering, Dry deposition loading of nitrogen to an alpine snowpack, Niwot Ridge, CO, in: *Biogeochemistry of Seasonal Snow-Covered Catchments*, IAHS press, publication no. 228, Wallington, UK, 1995, pp. 33–40.
- [10] J. Padro, Seasonal contrasts in modelled and observed dry deposition velocities of O₃, SO₂, and NO₂ over three surfaces, *Atmos. Environ.* 27A (1993) 807.
- [11] D.W. Stocker, K.F. Zeller, D.H. Stedman, O₃ and NO₂ fluxes over snow measured by eddy correlation, *Atmos. Environ.* 29 (1995) 1299.
- [12] A. Venkatram, P.K. Karamchandani, P.K. Misra, Testing a comprehensive acid deposition model, *Atmos. Environ.* 22 (1988) 737.
- [13] R.C. Bales, M.P. Valdez, G.A. Dawson, Gaseous deposition to snow: 2. Physical–chemical model for SO₂ deposition, *J. Geophys. Res.* 92 (1987) 9789.
- [14] S.L. Miller, Clathrate hydrates. Their nature and occurrence, in: *Phys. Chem. Ice Pap. Symp.*, R. Soc. Can., Ottawa, Ont, 1973, pp. 42–50.
- [15] P.W. Atkins, *Physical Chemistry*, 4th edn., Oxford Univ. Press, 1990, pp. 885–888.
- [16] M.H. Conklin, R.A. Sommerfield, S.K. Laird, J.E. Villinski, Sulfur dioxide reactions on ice surfaces: implications for dry deposition to snow, *Atmos. Environ.* 27A (1993) 2927.
- [17] R.A. Sommerfield, M.H. Conklin, K. Laird, NO adsorption on ice at low concentrations, *J. Coll. Interf. Sci.* 149 (1992) 569.
- [18] Colbeck, Grain clusters in wet snow, *J. Coll. Interf. Sci.* 72 (1979) 371.
- [19] D. Nenow, Surface premelting, *Prog. Cryst. Growth Character* 9 (1984) 185.
- [20] P. Zannetti, *Air Pollution Modelling. Theories, Computational Methods and Available Software*, Van Nostrand-Reinhold, New York, 1990.
- [21] W.A. Jury, W.F. Spencer, W.J. Farmer, Behavior assessment model for tracer organics in soil: I. model description, *J. Environ. Qual.* 12 (1983) 558.
- [22] R.J. Millington, Gas diffusion in porous media, *Science* 130 (1959) 100–102.
- [23] J. Crank, *The Mathematics of Diffusion*, Clarendon Press, Oxford, 1975, pp. 144–146.
- [24] E. Karlsson, Theoretical model for dry deposition of nerve agents to snow and water surfaces, Proceedings of the ERDEC Scientific Conference on Chemical Defense Research, 16–19 Nov. 1993, ERDEC-SP-024, U.S. Army Edgewood Research, Development and Engineering Center, 1993, pp. 407–413.
- [25] E. Karlsson, T. Berglund, M. Nordstrand, Deposition of sarin on snow, Proc. 5th Int. Symposium on Protection Against Chemical and Biological Warfare Agents, Stockholm, Sweden, 11–16 June 1995, National Defence Research Establishment, Department of NBC Defence, S-901 82 Umeå, Sweden, 1995, pp. 409–415.
- [26] AP2C Portative system for toxic agents detection, liquid and vapor form, GIAT industries, 78034 Versailles Cedex, France, 1997.
- [27] The Solent ultrasonic research anemometer, Gill instruments, Lymington, Hampshire, England, 1995.
- [28] W.J. Lyman, W.F. Reehl, D.H. Rosenblatt, *Handbook of Chemical Property Estimation Methods. Environmental Behaviour of Organic Compounds*, Am. Chem. Soc., Washington, DC, 1990.
- [29] J. Santesson, *Dictionary of Chemical Warfare Abbreviations, Acronyms and Colloquial Terms*, National Defence Research Establishment, Department of NBC Defence, S-901 82 Umeå, Sweden, 1984, p. 61.
- [30] P.H. Howard, W.M. Meylan, *Handbook of Physical Properties of Organic Chemicals*, CRC Lewis Publishers, 1997, p. 181.
- [31] M.C. Johnson, *Methodology for Chemical Hazard Prediction*, Department of Defence Explosives Safety Board, Alexandria, VA, USA, AD-A086820, 1980.
- [32] A FOA Briefing Book on Chemical Weapons, National Defence Research Establishment (FOA), S-17290 Stockholm Sweden, 1992, p. 24
- [33] C. Bernes, Nordens miljö-tillstånd, utveckling och hot, monitor 13, Naturvårdverket, S-171 85 Solna Sweden, 1993, p. 41.
- [34] *Chemical Warfare Agents, and Related Chemical Problems*, Vol. 1, Parts 1–2, National Technical Information Service, PB_158 508, 1946.

- [35] N. Forman, H. Frostling, O. Hertzberg, B. Jansson, L. Larsson, J. Lundin, A. Meyerhöffer, G. Persson, J. Santesson, B. Sörbo, B. Östman, C-stridsmedlen. Egenskaper och skydd. Supplement till FOA orienterar om BC-stridsmedel, National Defence Research Establishment, Department of NBC Defence, S-901 82 Umeå, Sweden, 1975, p. 2:1.
- [36] W. Blumberg, E.-U. Schlünder, Simultaneous vapor and liquid diffusion in partially wetted porous media, *Drying Technol.* 11 (1) (1993) 41–46.